The effect of Volume Expansion on the Propagation of Wrinkled Laminar Premixed Flame

E.H. Chung and Sejin Kwon

Department of Aerospace Engineering, KAIST,373-1 Kusong-dong, Yusung-ku, Taejon 305-701, Korea

ABSTRACT

Under certain circumstance, premixed turbulent flame can be treated as wrinkled thin laminar flame and its motion in a hydrodynamic flow field has been investigated by employing G-equation. Past studies on G-equation successfully described certain aspects of laminar flame propagation such as effects of stretch on flame speed. In those studies, flames were regarded as a passive interface that does not influence the flow field. The experimental evidences, however, indicate that flow field can be significantly modified by the propagation of flames through the volume expansion of burned gas. In the present study, a new method to be used with G-equation is described to include the effect of volume expansion in the flame dynamics. The effect of volume expansion on the flow field is approximated by Biot-Savart law. The newly developed model is validated by comparison with existing analytical solutions of G-equation to predict flames propagating in hydrodynamic flow field without volume expansion.

To further investigate the influence of volume expansion, present method was applied to initially wrinkled or planar flame propagating in an imposed velocity field and the average flame speed was evaluated from the ratio of flame surface area and projected area of unburned stream channel. It was observed that the initial wrinkling of flame cannot sustain itself without velocity disturbance and wrinkled structure decays into planar flame as the flame propagates. The rate of decay of the structure increased with volume expansion. The asymptotic change in the average burning speed occurs only with disturbed velocity field. Because volume expansion acts directly on the velocity field, the average burning speed is affected at all time when its effect is included. With relatively small temperature ratio of 3, the average flame speed increased 10%. The combined effect of volume expansion and flame stretch is also considered and the result implied that the effect of stretch is independent of volume release.

1. INTRODUCTION

The phenomenon of turbulent flame involve nonlinearities in the governing equations that arise from convection process and reaction sources and direct solution of the problems with and practically does not seem to feasible in near future. Sivashinsky (1979) has proposed an alternative method of flame propagation simulation using the laminar flamelet assumption. In this method, flame is treated as a wave which propagates with a laminar burning velocity normal to the flame surface while the surface is advected by the flow as a material interface. Reaction is decoupled from the equation and influences the flame propagation through laminar burning velocity(S_u) only. Instantaneous flame motion can be simulated by solving the flow field and moving the flame surface subjected to burning into the unburned zone in addition to the flow motion. Thin laminar flamelet is a valid assumption in a wide range of fuels and Reynolds numbers despite its rather strict requirement.

Recent development in this area of research includes Ghoniem et al.(1982), Chorin(1980), Sethian(1984), Osher and Sethian(1988) and Kwon et al.(1992). Ghoniem et al. User random vortex method for turbulence simulation and Chorin's algorithm for flame propagation. Kwon et al. Used stochastic time series technique to simulate isotropic turbulence and SLIC(Simple Line Interface Calculations, Noh and Woodward, 1976) for flame propagation algorithm. Kwon and Faeth(1992) further extended the method to predict three dimensional turbulent premixed flame propagation in a fan-stirred spherical combustion bomb, using G-equation for flame propagation algorithm.

Kerstein et al.(1988) and Osher and Sethian(1987) acknowledged that an equation of Hamilton-Jacobi type for wave motion could be used in flame propagation in a premixed gas. The equation is known as G field equation to emphasize the distribution field of G values while the equation that governs its motion arises from the Lagrangian description of a material surface defined by level surface of G. The only physically relevant information of G is its level curve representing the flame front and its gradient at that curve that points into the unburned gas region normal to the tangent of the curve. Other than that, we have freedom to choose any functional form of G distribution. It must be stressed that G has different origin from the reaction progress variable of Bray(1980) and should not be interpreted such in evaluation other properties. G-equation has replaced previous flame propagation algorithms such as SLIC, because it is mathematically sound and relatively easy to implement in more complex problems.

Aldredge (1992) studies steady flame propagation in the periodic shear field and included the effect of flame stretch. Zhu and Ronney(1994) simulated flame in Taylor-Couette flow and reported agreement between prediction and measurement of liquid flames where there was no density difference across the flame front. Sung et al. (1996) modified G-equation using its gradient and obtained analytic solution of flame propagating into quiescent reactant region neglecting the density change at the flame.

Numerous investigators studied the interaction of flame and elementary turbulence, namely, fixed vortices(Ashurst, 1995) of flow field(Ashurst and Sivashinsky, 1991) using G-equation. To extend this model to practical problems, it is required to include all the known mechanism that influences flame dynamics. For example, the model should accommodate the effect of flame stretch, volume expansion and preferential diffusion. The advantage of using G-equation in premixed flame is that it is relatively easy to include these additional mechanisms into the model. Sung et al. (1992) and Zhu and Ronney(1994) included the effect of flame stretch in the model and showed how the local flame stretch affects the overall burning speed. Both of the studies assumed constant density field and neglected the density discontinuity across the flame front. It is well known that volumetric expansion significantly modifies the flow field of the unburned gas mixture of combustion bomb. The effect of volume expansion deflects the streamline away from the centerline in the burned region of premixed jet flame issuing into open atmosphere.

2. THEORETICAL METHOD

Assumptions for the analysis are; flame is in thin laminar flamelet regime and approximated infinitely thin surface that divides the flow field into burned and unburned region(1), within the burned and unburned region, the gas is treated as incompressible(2), reaction is instantaneous at the flame surface and the gas mixture experiences volume expansion due to reaction heat(3) and finally, the volume expansion occurs only at the flame front and modifies the flow field as volume sources(4).

Consider a scalar function $G(\vec{r},t)$, whose level surface, $G(\vec{r}_f,t)=0$, represent flame surface within the thin laminar flamelet regime. Taking the time derevative of the level surface equation, following equation that governs flame surface motion is obtained,

$$\left.\frac{dG}{dt}\right)_{G=0}=\frac{\partial G}{\partial t}+\frac{d\vec{r}_f}{dt}\cdot\nabla G=0 \tag{1}$$

where the propagation velocity, $d\vec{r}_f/dt$, appears explicitly. S_u is local laminar burning velocity normal to the flame surface and is defined by

$$S_u = \left(\frac{d\vec{r}_f}{dt} - \vec{v} \right) \cdot \hat{n}_f \qquad (2)$$

where S_u is the velocity of the unburned gas at the flame front and $\hat{n}_f = -\nabla G / |\nabla G|$ is the unit normal vector into the unburned region at the flame surface. Elimination $d\vec{r}_f / dt$ from Eqs.(1) and (2), one obtains the well known form of G-equation.

$$\frac{\partial G}{\partial t} + \vec{v} \cdot \nabla G = S_u |\nabla G| \qquad (3)$$

$S_u |\nabla G|$ represents active combustion wave propagation abd moves the flame surface in accordance with Huygens' principle. Convection term accounts for passive interface advection in the imposed flow field. On the other hand, the Lagrangian description of flame surface motion by Ghoniem et al. is as follows,

$$\frac{d\vec{r}_f}{dt} = \vec{v} + S_u \hat{n}_f \qquad (4)$$

where $\vec{v}$ means flame advection due to the neighboring velocity field and $S_u \hat{n}_f$ means self-propagation of flame front. Multiplying $-\nabla G$ to eq. (4) and using the definition of $\hat{n}_f$, we obtain

$$-\frac{d\vec{r}_f}{dt} \cdot \nabla G + \vec{v} \cdot \nabla G = S_u |\nabla G| \qquad (5)$$

Thus, Eq. (3) and Eq. (5) are equivalent if we use Eq. (1), i.e. G-equation in the Eulerian view point and flame propagation equation in the Lagrangian point are equivalent each other.

Fig. 1 is a schematic of a stationary planar flame to show the velocity adjustment in the burned region by volumetric expansion at the flame surface. Continuity across a unit flame surface area requires

$$\rho_b S_b = \rho_u S_u \qquad (6)$$

The adjusted velocity field can be simulated by distributing volume source elements of source strength $(\nu - 1)S_u$ along the flame front, where ν represents density ratio of unburned and burned gas and is equivalent to temperature ratio of burned and unburned gases.

$$\frac{\rho_u}{\rho_b} = \frac{T_b}{T_u} \equiv \nu \qquad (7)$$

For low subsonic burning velocities, the influence of pressure is negligible and newly generated volume per unit time and unit flame length is as follows,

$$S_b - S_u = (\nu - 1)S_u \qquad (8)$$

Fig. 2 is a schematic of velocity induced by line volume source segment with source strenth as definde in previous section. The volume source is distributed on the wrinkled flame sruface and depending on the orientation of the small line segment of the flame surface, velocity potential increment by infinitesimally small line volume source segment is written as

$$d\phi = \frac{S_u(\nu - 1)}{2\pi} \ln\sqrt{(x_p - s)^2 + y_p^2} \cdot ds \tag{9}$$

By integrating Eq. (9) over the flame segment length, following velocity potential is obtained.

$$\Delta\phi = \frac{S_u(\nu - 1)}{2\pi} \int_{S_1}^{S_2} \ln\sqrt{(x_p - s)^2 + y_p^2} \cdot ds \tag{10}$$

Eq. (9) represent the velocity potential induced by a single line source element and corresponding velocity component is

$$v_p = \left.\frac{\partial\phi}{\partial x}\right)_p = \frac{S_u(\nu - 1)}{2\pi} \ln\left(\frac{\sin\theta_2}{\sin\theta_1}\right) \tag{11}$$

$$v_n = \left.\frac{\partial\phi}{\partial y}\right)_p = \frac{S_u(\nu - 1)}{2\pi} (\theta_2 - \theta_1) \tag{12}$$

Summing the contributions of all the flame segments and superimposing to the mean velocity field of unburned gas region can simulate complete velocity field.

3. NUMERICAL METHODS

3.1 Decretization

Eq. (1) is discretized in a follwing way. Over each time step, G field is updated by simultaneously by Eq. (13) and (14) using operator splitting technique. Let the solution of Eq. (13) $G_{i,j}^{n+1,*}$ and the right hand side of Eq. (14) $H_{i,j}$. Then, $G_{i,j}^{n+1}$ is evaluated from existing distribution and velocity filed by

$$G_{i,j}^{n+1} = G_{i,j}^{n+1,*} + \Delta t \cdot H_{i,j} \tag{13}$$

Equidistanced($\Delta x = \Delta y = h$) staggered grid system was used. At the upstream and downstream boundaries, dummy cells were used to specify boundary conditions for G by extrapolation, while reflection condition provided satisfactory boundary values in the sides.

The overall scheme becomes explicit and requires the time step to satisfy the Courant-Friedrichs-Lewy condition, that is

$$\Delta t \cdot \max\left(\frac{|u_{i,j}|}{h}, \frac{|v_{i,j}|}{h}, \frac{S_u}{h}\right) \le 1 \tag{14}$$

To account for the effect of volume expansion, it is required that the location of flame front must be specified. This poses a task of extracting a level curve of $G = 0$ from the distribution of G values. When the G changes signs over one grid spacing, the flame location was found by linear interpolation. Here we assumed the grid system is sufficiently fine so that flame front crosses a cell boundaries at only two distinct points except cusp locations.

Beginning at an appropriate boundary, each cell is examined whether G changes signs across the cell. Once a cell is found to contain flame front, use the interpolation to calculate the approximate coordinate of flame crossing from the G values at the grid points and proceed neighboring cells which share the side wall where flame passes with the previous cell. In this way, flame surface location can be found without examining the whole grid points in the domail of compututation.

After all the points on the flame surface is found, a flame segment is approximated by a line connecting neighboring two points and each segment is assigned a volume source with the source strength as defined in Eq. (8). The induced velocity field is reevaluated by eq. (11) and (12). By superimposing the induced velocity field onto the mean velocity field of upstream, complete velocity field is obtained and the combined velocity field changes at each computational time step.

3.2 G-redistribution technique

When there is no volume expansion, the velocity field is externally imposed and maintains itself throughout the flame propagation. Although it is not a realistic model, the invariance of velocity field simplifies the task of G value distribution as the basic profile of G-distribution is also invariant within such flow field. Fig. 3 shows the behavior of G field in a uniform velocity field. The profile of G-distribution does not dissipate or disperse along the axis of propagation and requires no special treatment. However, volumetric expansion along a wrinkled laminar flame front induces velocity field which is neither uniform nor steady. As a result, G profile changes shapes as the flame propagates into the unburned region and influences the self-propagation part of Eq. (3). At this point, it must be noted that G-function is a purely mathematical representation of flame front and its only physical information is the location of flame surface and the direction of self-propagation. The arbitrary velocity field induced by volume expasion modifies G-profiles such that its maximum gradient points different direction from the surface normal vector of the flame. The solution becomes divergent by the accumulation of the unsteadiness in the flow field. To avoid this problem, G-distribution in redefined after each time step so that it maintains the initially provided profile in the immediate vicinity of the flame surface. Because the location of flame which is defined by

$y = f(x,t)$ is not affected by the modified velocity unless one full tome step is proceeded, G is redistributed by $G(x,y) = y - f(x,t)$. In actual calculation, G values are needed only within a narrow region that contains flame surface. The idea is also relevant to the fact that the origin of G-equation is a Lagrangian description of flame front as in Eq. (4).

3.3 The Effect of Flame Stretch

To test present model, flame stretch is considered in addition to volume expansion. Flame stretch participates in the flame surface dynamics through laminar flame speed adjustment. Experimental evidance shows that local laminar flame speed S_u can be correlated to the flame stretch by (4)

$$S_u = S_L(1 - \varepsilon\kappa) \tag{15}$$

, where S_L is laminar flame speed of planar flame without stretch, κ is dimensionless flame stretch and defined by flame surface geometry, while ε is not a property of flow field but of gas mixture and defined by flame thickness(δ) and Markstein length scale(L) by $\varepsilon = (\delta / l)(L/\delta)$. Flame stretch is a combined effect of curvature of the flame and strain of flow field and its general formulation is as follows according to,

$$\kappa = -(\nabla \cdot \hat{n} + \hat{n} \cdot \tilde{e} \cdot \hat{n}) \tag{16}$$

with unit surface normal vector ($\hat{n}$) of the flame and the velocity strain field ($\tilde{e}$). Using G to express Eq. (18) in Cartesian coordinate system,

$$\kappa = -\frac{G_{xx}G_y^2 - 2G_{xy}G_xG_y + G_{yy}G_x^2}{|\nabla G|^3} - \frac{\alpha(G_x^2 - G_y^2) + 2\beta G_xG_y}{|\nabla G|^2} \tag{17}$$

where nondimensional local rate-of-strain tensor is given by

$$e = -\frac{1}{2}\left[(\nabla\vec{v}) + (\nabla\vec{v})^T\right] = \begin{pmatrix} \alpha & \beta \\ \beta & -\alpha \end{pmatrix} \text{ where } \alpha = u_x, \beta = \frac{u_y + u_x}{2} \tag{18}$$

At each time step a new laminar flame speed is evaluated locally by Eq. (17) and substituted into Eq. (3) to see the influence of flame stretch on the flame dynamics.

4. RESULTS

Three initial shapes of flame front were tried to understand the effect of volume release in a quiescent gas mixture and prescribed mean flow field of sinusoidal velocity distribution. At t = 0, the initially imposed flames are defined by $y = f(x, t = 0) = 0, A\cos x, -A\cos x$. The sinusoidal velocity distributions have been studied in connection with elementary flame-vortex interaction problems such as in

Ashurst(1991) and Sung et al.(1996). The initial distribution of G was specified by $G(x, y, t = 0) = y - f(x,0)$ and flame propagates in opposite direction of y-axis. If the laminar flame speed is invariant, the ratio of average burning speed U_t and the laminar speed is equivalent to the ratio of flame surface area and the cross sectional area of the flow field, that is 2π in the present study.

In Fig. 4(a), the average burning speed of a flame with cosine shape in quiescent gas mixture was plotted against analytical solution(Sung et. al., 1996). Numerical calculation of present study shows excellent agreement with the theory. Because of the initial disturbance of flame shape, U_t begins around 1.22 and approaches 1 as the wrinkling smoothes out due to flattening effect of self-propagation mechanism. Fig. 5 shows that flame forms a cusp as it propagates and eventually the cusp disappears with overall flattening of the wrinkled flame unless there is additional wrinkling process. In Fig. 4(b), the imposed velocity field is $\vec{v} = (0, A\cos x)$. Initially planar and sinusoidal flame propagation in the velocity field was compared by U_t/S_L, neglecting the effect of volume expansion. Present calculation agrees very well with theory and the average flame speed approaches the same asymptotic value of 2.0 regardless of its initial shape. This implies that the flow field rather than the initial wrinkling control eventual shape of the flame. It can be explained by the fact that flow field constantly distorts the flame while the initial wrinkles die away quickly as observed in Fig. 5.

Fig. 6 shows the influence of volume expansion on the average flame speed U_t with initial wrinkling in a quiescent flow. As discussed in previous section, the average burning speed approaches laminar burning speed of given mixture fraction in uniform velocity field regardless of the shape and magnitude of the initial wrinkling. However, in early stage of flame propagation while there is remaining surface distortion, volume expansion definitely influences the average flame speed. As the temperature ratio of burned and unburned gas (T_b/T_u) increases from 1 to 2, 3 and 4, the influence becomes more pronounced. This behavior is also observed in Fig. 5 where the flame shapes were plotted at different time steps for each temperature ratio. For the cases involving volume expansion, the results were plotted along with no volume release for comparison. With increasing temperature ratio, the flame flattens out more quickly implying accelerated average flame speed, which corresponds to the observation made earlier in Fig. 6.

The effect of volume expansion in a prescribed periodic flow field is shown in Fig. 7. The planar and sinusoidal shapes of initial flame wrinkling were tried and the resulting average burning speed was plotted along with cases of Fig. 4 that is without volume expansion. As in the case without volume expansion, the mean flow field determines the eventual wrinkling. Volume expansion appears to interfere with the asymptotic flame shape and it has a lasting influence on the average flame speed as shown in the figure. The effect of volume release is expected to increase with higher temperature ratios. Fig. 8 represents the flame fronts at different time steps and the eventual shape of the flame is independent of the initial wrinkling. The overall effect of volume expansion is to make the cusps sharper and increase the average burning speed as results because sharper cusps increase the flame surface area.

The effect of the flame stretch is shown in Fig. 9 for initially wrinkled flames in a quiescent gas mixture. The asymptotic behavior of flame was independent of stretch parameter ε as its value changed from 0 to 0.09. In all the cases tested, the flame flattens out after sufficient time passes and eventually planar laminar speed was attained. In early stage of flame propagation while the flame still maintains sizable wrinkles, the effect of higher stretch parameter slows down the mean flame speed down by up to 10% but approaches asymptotic speed faster than the case of low values of stretch parameters. The larger the stretch parameter, the faster the stretch effects attenuate the wrinkled structures of flame geometry. This tendency remains even when the volume expansion is considered simultaneously as in Fig. 10. Fig. 10(b) manifests reduced depth of wrinkling especially near the cusp point when compared with Fig. 10(a), which experiences no stretch.

5. CONCLUDING REMARKS

In the present study, a method was developed to include the effect of volume expansion in the description of the flame front dynamics using G-equation and the modified flow field by volume expansion was observed. The newly developed model was verified by comparison with analytical solutions of flame propagation in the imposed flow field neglecting volume expansion. With volume expansion included, the flow field is adjusted to accommodate increased volume flow rate crossing the flame front and the resulting streamline predicts the same behavior of measured streak line qualitatively.

To further investigate the influence of volume expansion, present method as applied to initially wrinkled or planar flame propagating in an imposed velocity field and the average flame speed was evaluated from the ratio of flame surface area and flat projected area of stream channel. It was observed that the initial wrinkling of flame could not sustain itself without velocity disturbance and wrinkled structure decays into planar flame. The asymptotic change in the average burning speed occurs only with disturbed velocity field. Because volume expansion acts directly on the velocity field, the average burning speed is affected by including the volume expansion at all times. With relatively small temperature ratio of 3, the average flame speed increased 10%.

References

Aldrege, R. C. (1992) The Propagation of Wrinkled Premixed Flames in Spatially Periodic Shear Flow. Combust. Flame, 90, 121-133.

Ashurst, W. T. and Sivashinsky, G. I. (1991) On Flame Propagation through Periodic Flow Fields. Combust. Sci. Tech., 80, 159-164.

Ashurst, W. T. (1995) A Simple Illustration of Turbulent Flame Ball Growth. Combust. Sci and Tech., 104, 19-32.

Bray, K. N. C. (1980) Turbulent Flow with Premixed Reactants. Turbulent Reacting Flows, P. A. Libby and F. A. Williams, eds., pp.115-184.

Chorin, A. J. (1980) Flame Advection and Propagation Algorithms. J. Comp. Phys., 35, 1-11.

Ghoniem, A. F., Chorin, A. J., and Oppenheim, A. K. (1982) Numerical Modeling of Turbulent Flow in a Combustion Tunnel. Phil. Trans. R. Soc. Lond. A-304, 303-325.

Kerstein, A., Ashurst, W. T. and Williams, F. A. (1988) Field Equation for Interface Propagation in an Unsteady Homogeneous Flow Field. Phys. Rev. A., 37, 2728.

Kwon, S., Wu, M. S., Driscoll, J. F. and Faeth, G. M. (1992) Flame Surface Properties of Premixed Flames in Isotropic Turbulence: Measurements and Simulations. Combust. Flame, 88, 221-238.

Kwon, S. and Faeth, G. M. (1992) Laminar Burning Velocities and Transition to Unstable Flames in $H_2/O_2/N_2$ and $C_3H_8/O_2/N_2$ Mixtures. Combust. Flame, 90, 230-246.

Noh, W. T. and Woodward, P. (1976) SLIC, Simple Line Interface Calculations. International Conference on Numerical Methods in Fluid Dynamics, A. I. Vooren and P. J. Zandenbergen, eds., Springer-Verlag, pp.330-339.

Osher, S. and Sethian, J. (1988) Front Propagation with Curvature-Dependent Speed: Algorithm Based on Hamilton-Jacobi Formulations. J. Com. Phys., 79, 12.

Sethian, J. (1984) Turbulent Combustion in Open and Closed Vessels, J. Com. Phys., 54, 425-456.

Sivashinsky, G. I. (1979) Hydrodynamic theory of flame propagation in a enclosed volume. Acta. Astronautica, 6, 631.

Sung, C. J, Yu, K. M., and Law, C. K. (1992) On the Geometry and Burning Intensity of Wrinkled Premixed Flames. AIAA Paper 92-0238.

Sung, C. J., Sun, C. J., and Law, C. K. (1996) Analytic Description of the Evolution of two-dimensional Flame Surfaces. Combust. Flame, 107, 114-124.

Zhu, J., and Ronney, P. D. (1994) Simulation of Front Propagation at Large Nondimensional Flow Disturbance Intensities. Combust. Sci. Tech, 100, 183-201.

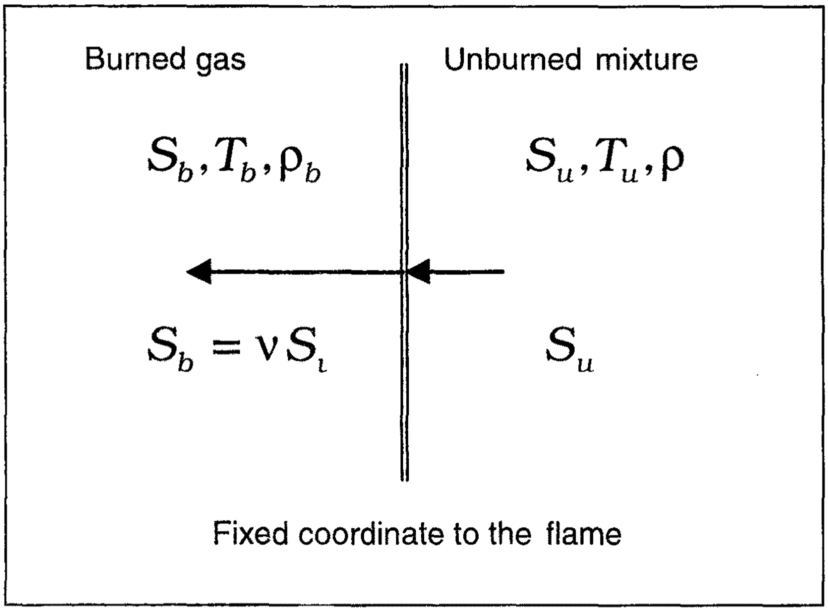

Fig. 1 Concept of volume expansion effect in 1-dimensional flame propagation

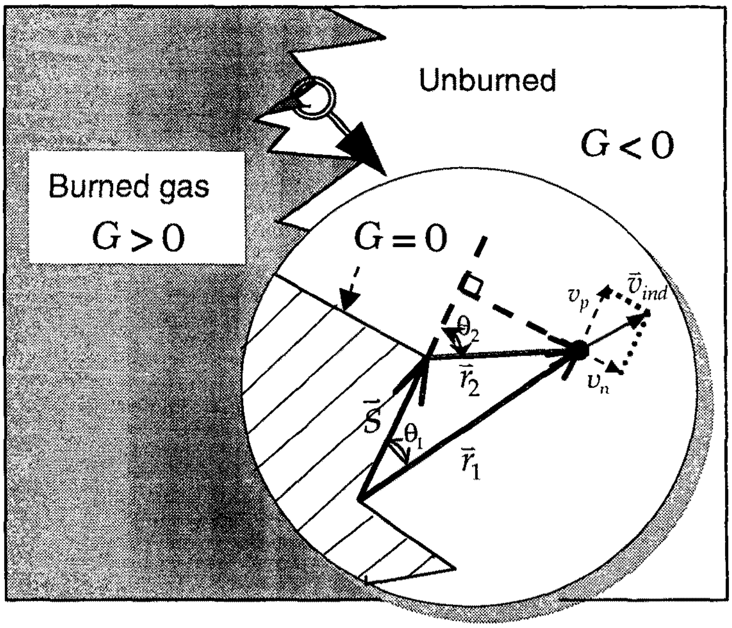

Fig. 2 Schematic diagram of thin flame surface where line volume source is assigned to obtain in
velocity

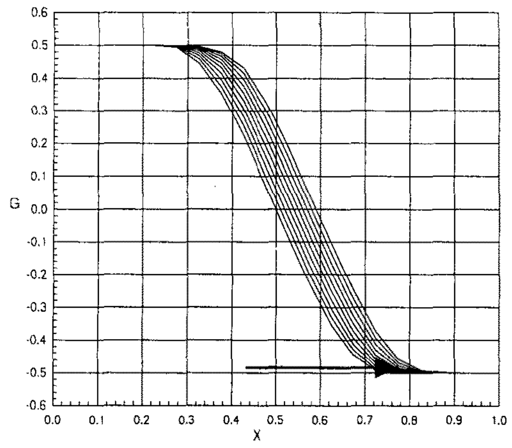

Fig. 3 Linear advection of flame front w/t self-propagation

(U=0.5, Su=0.5, t=0.00 ~ 0.10, dt=0.01)

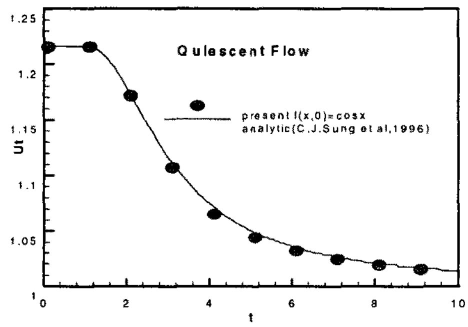

(a)

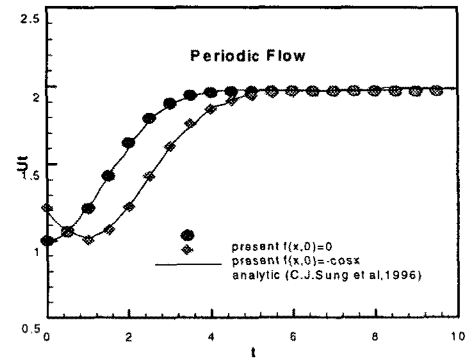

(b)

Fig. 4 Average flame speed in (a) quiescent flow and in (b) peric c flows shapes where f(x,0) is the initial flame shape

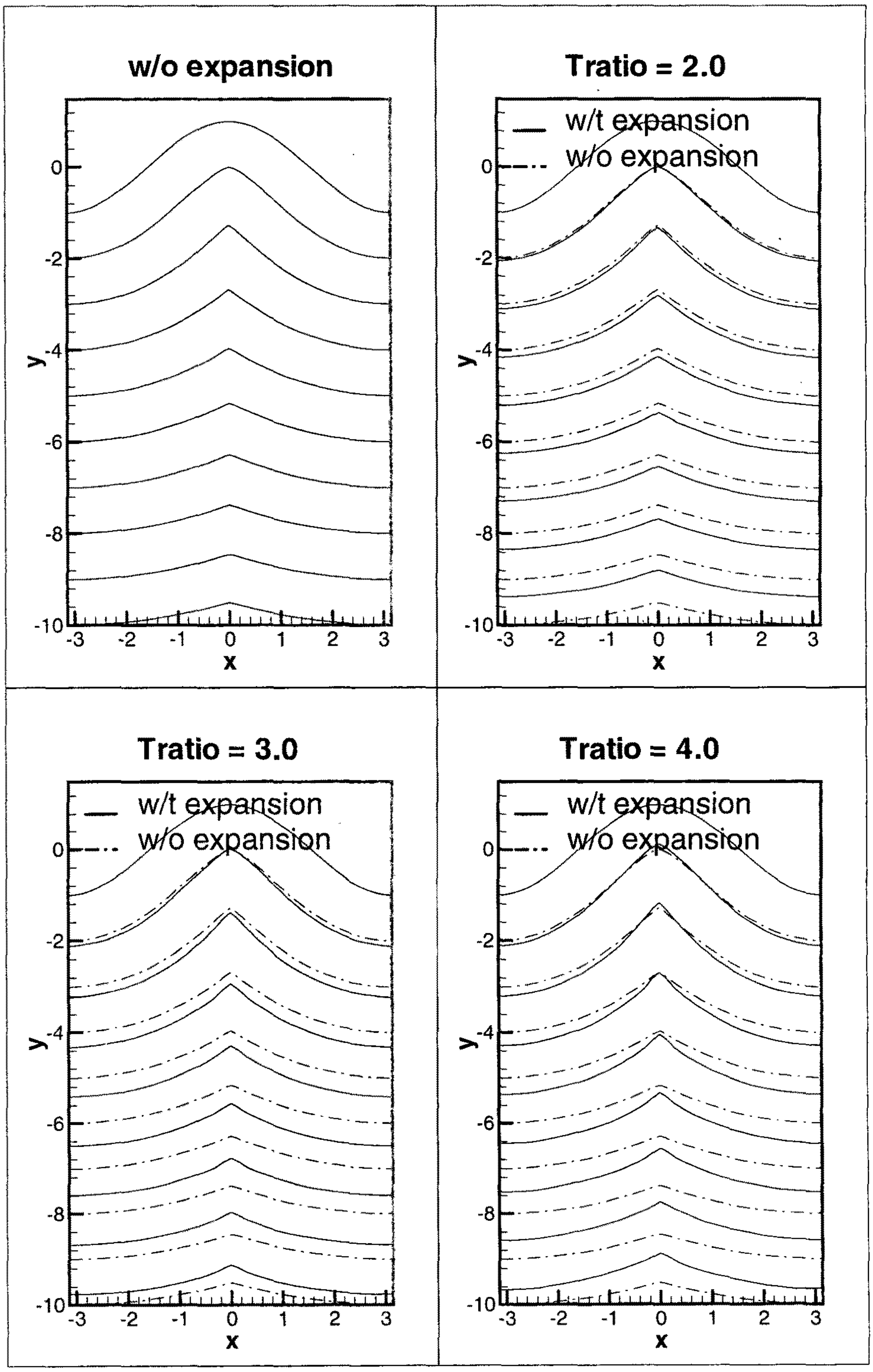

Fig. 5 Flame propagation without/with thermal expansion effect in quiescent flow

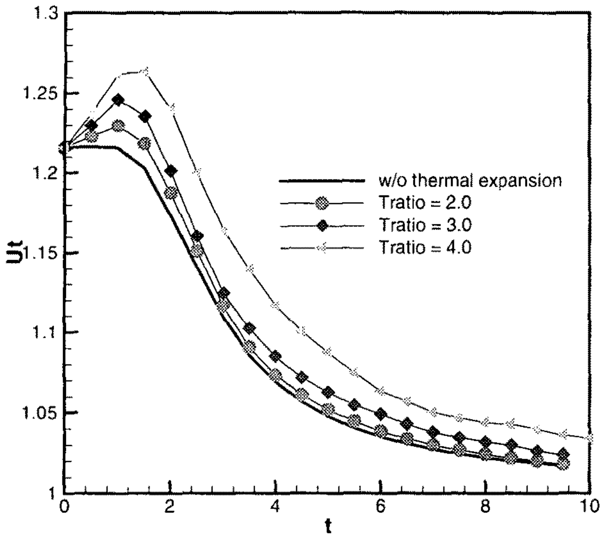

Fig. 6 Thermal expansion effect for initially quiescent flow field for temper

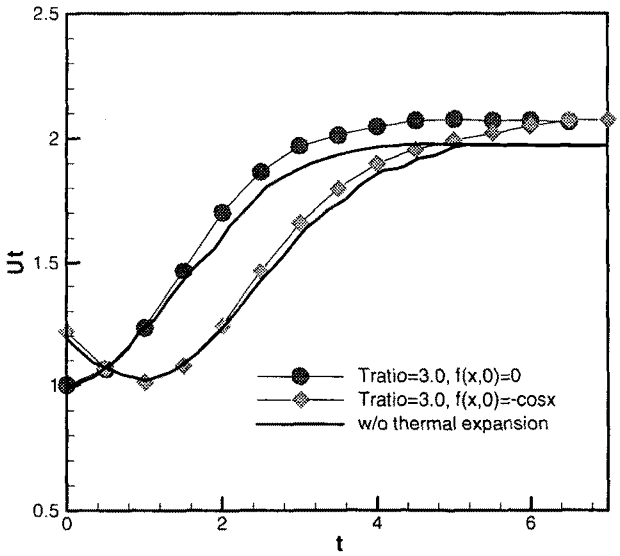

Fig. 7 Flame propagation w/t and w/o thermal expansion in periodic flow

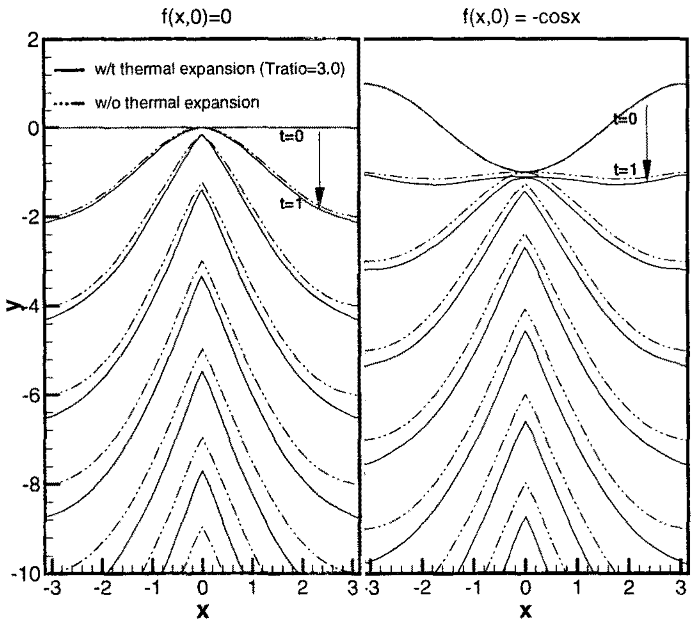

g. 8 Flame propagation without/with thermal expansion effect in periodic flow

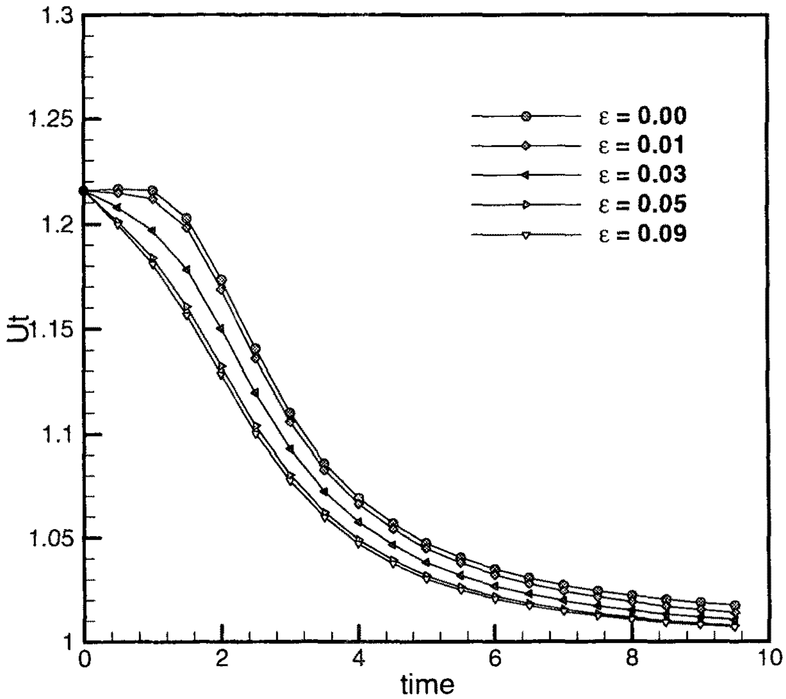

Fig. 9 Stretch effect on average flame speed in quiescent flow

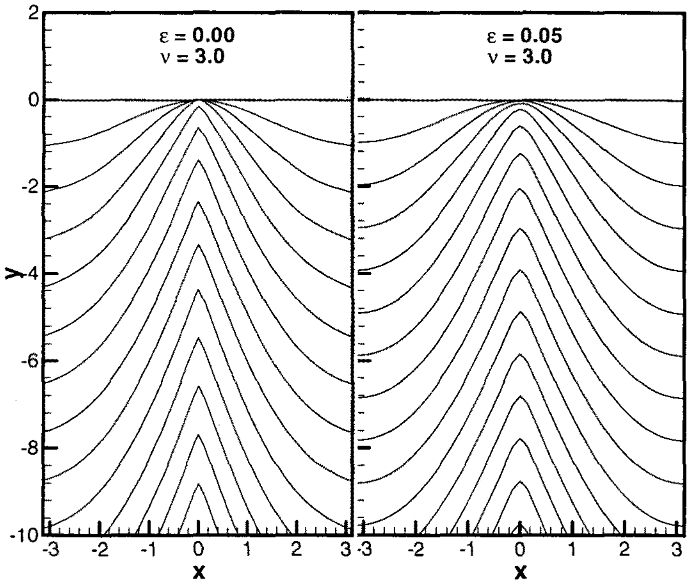

ne propagation without/with stretch effect w/t thermal expansion in pe